Research Report

Application of Stochastic Resonance to Improve the Performance of Pedestrian-recognition Systems in Halation Environments

Yukihiro Tadokoro, Seiya Kasai, Akihisa Ichiki and Hiroya Tanaka

∎**ABSTRACT**‖ To date, a variety of night-vision systems and related devices have been proposed or developed to assist drivers in identifying pedestrians at night. By improving the hardware and software algorithms in these devices, it should be possible to design systems that can achieve a required recognition performance. In this study, we focus on stochastic resonance, which offers the peculiar and counterintuitive effect that by adding noise to a system, exceedingly weak signals and information can be amplified. We propose and evaluate a simple technique that realizes the required recognition performance with no need to redesign devices or other components. The scenarios we consider are halation environments; by fabricating a simple prototype device and conducting experiments designed to mimic real-world situations, we demonstrate the possibility of improved recognition performance in halation environments through the application of stochastic resonance. In comparison with auto-gain control (AGC) – another method used to improve performance in environments of this type – we demonstrate that our proposed method offers the advantage of improving the dynamic range of a system, a feature not offered by existing AGC techniques.

∎**KEYWORDS**‖ Stochastic Resonance, Image Sensor, Dynamic Range

1. Introduction

Efforts to assist drivers in recognizing pedestrians at night have resulted in the proposal and development of night-vision systems and a variety of similar devices. By improving the hardware and software algorithms in these devices, it should be possible to design systems that can achieve a required recognition performance. In this study, we propose and evaluate a simple system for realizing the required performance with no need to redesign devices or other components. Our proposal is based on an application of the concept of stochastic resonance, a phenomenon characterized by the peculiar and counterintuitive feature that by adding noise to a system, exceedingly weak signals and information can be extracted.

The term "stochastic resonance" refers to a class of phenomena involving optimized responses to weak signals arising from noise. The human brain, the human visual sensory system, and other biological organs and mechanisms exhibiting nonlinear characteristics may be said to involve stochastic resonance.[1-4] The application of stochastic resonance to information-related devices offers the possibility of allowing the detection of weak signals that could not be detected using previous methods. More specifically, on the basis of theoretical arguments and a variety of other considerations, it is known that these methods offer the following two advantages in practical applications.

First, weak signals to which a given system cannot respond may become observable through the intentional addition of an appropriate amount of noise. Any given device has its own dynamic range, and the device is incapable of responding to weak signals lying outside this range. In this case, the dynamic range can be improved by adding an appropriate amount of noise, creating the possibility of detecting tiny sub-threshold signals or strong signals that could not be detected given the usual performance of the device.[3-8]

A second practical advantage is that, in environments characterized by a low signal-to-noise ratio (SNR), weak signals may be recovered by a stochastic resonance based filter. A low SNR corresponds to a situation in which a signal that could be readily detected in the absence of noise is buried beneath noise with a magnitude much larger than that of the signal; in such cases it is difficult to recover the signal. If, in

a situation of this sort, the noise exhibits non-Gaussian characteristics, then an optimally-designed nonlinear filter exhibiting stochastic resonance can extract the weak signal with greater accuracy than traditional methods such as linear filters.[9-13]

To date, stochastic resonance phenomena have been considered primarily within the field of nonlinear physics; we are not aware of any examples of practical applications. Here, we fill this gap by reporting the results of a successful application of stochastic resonance, which exploits the first of the above advantages, in a real-world application involving automobiles. As shown in **Fig. 1**, the situation we consider is one in which pedestrians are effectively invisible to drivers due to glare and halation at night. In night-vision systems that assist drivers in recognizing pedestrians, the intense light emitted by headlights may saturate the detection devices, resulting in degraded performance. Techniques such as auto-gain control (AGC) may be considered in order to address this difficulty; however, AGC does not actually increase the dynamic range of a detector (the range of input light intensity to which the device can respond), but rather simply shifts it in the direction of higher-intensity signals. This has the drawback of rendering the system incapable of responding to low-intensity signals. In the application of stochastic resonance we propose here, the simple procedure of adding noise not only has the effect of shifting the dynamic range toward high-intensity signals, but actually increases the dynamic range. We have fabricated a prototype device to validate our proposed method; in this paper we present a theoretical analysis and visual validation of the effects described above.

Fig. 1　Example of a pedestrian under glare conditions from the driver's viewpoint.

2. Prototype Device Circuit and the System

Figure 2 schematically illustrates the test system we constructed, including the fabricated prototype device. To mimic the situation shown in Fig. 1 in a laboratory, we used an LED light source in place of automobile headlights. We represented the effect of a pedestrian walking in front of a headlight by hand-waving a transparent OHP sheet, on which was printed an image of a pedestrian, in front of the LED light. The portion of the sheet containing the printed image decreases the light by an amount A lx; thus, below a certain LED light intensity, the shape of the image may be recognized by the human eye. However, because our test setup involves only a short distance between the LED light and the sheet, the received light intensity is high. This gives rise to the glare phenomenon depicted in Fig. 1 and prevents identification of the shape of the pedestrian.

Our test setup reproduces the way in which the human eye experiences this glare. The image-sensor portion uses a photodetector (PD)[14] to receive the light signal and convert it to an electrical signal; this signal is then visualized using an LED array[15] installed in the display portion of the setup. In our test system we alternately turn the LED on and off to ensure that the image of the pedestrian is properly reproduced for the appropriate light intensity; however, under high light intensity the PD and LED output are saturated and the shape of the image is not properly reproduced. This corresponds to the situation shown in Fig. 1, where a human cannot recognize a pedestrian. As discussed in Sec. 3. 1, the LED and, not the PD, is in fact saturated. To increase the resolution of our system, we constructed 10×10 arrays of PDs and LEDs, as shown in **Fig. 3**.

Based on this system, we propose a method to enhance shape recognition by exploiting stochastic resonance. Our goal was to extract the shape of a pedestrian – a weak signal in the presence of high-intensity light – by adding an appropriate amount of noise, thus realizing the practical advantage discussed in Sec. 1. To this end, we added an appropriate amount of noise to devices in our test setup. This mimics the effect of glare, and by using stochastic resonance to improve the dynamic range of the PD, we avoid the large input voltages that cause saturation of the LED display. Because the PD characteristics vary with the operating voltage V_p[14], we chose to add noise

to this voltage. More specifically, we used a function generator as a voltage source; this source produced a driving voltage of $V_p = V_c + V_\eta$, where V_c is a fixed offset voltage and V_η is a noise signal. For the noise signal we used easily-generated white Gaussian noise with a mean of zero and a variance of σ_η^2. Thus, the probability distribution for the driving voltage V_p is

$$P(V_p) = \frac{1}{\sqrt{2\pi\sigma_\eta^2}} \exp\left\{-\frac{(V_p - V_c)^2}{2\sigma_\eta^2}\right\} \qquad (1)$$

and various driving voltages, centered around V_c, appear stochastically. Because stochastic resonance depends on the noise power, the variance term (noise power) σ_η^2 in Eq. (1) must be adjusted to an appropriate value.

3. Performance Analysis

In this section we analyze the performance of our proposed prototype device. First, in Sec. 3. 1 we discuss the results of measurements performed to determine the basic properties of the circuit, and we illustrate the operation mechanism and the nature of saturation in our prototype device. In Sec. 3. 2, we present a theoretical derivation of the properties of the system in the presence of noise added to the driving voltage.

3. 1 Basic Performance of the Prototype Device

Here, we describe the operating principles of the device based on Fig. 2, as well as measurement results, to investigate the conditions under which saturation
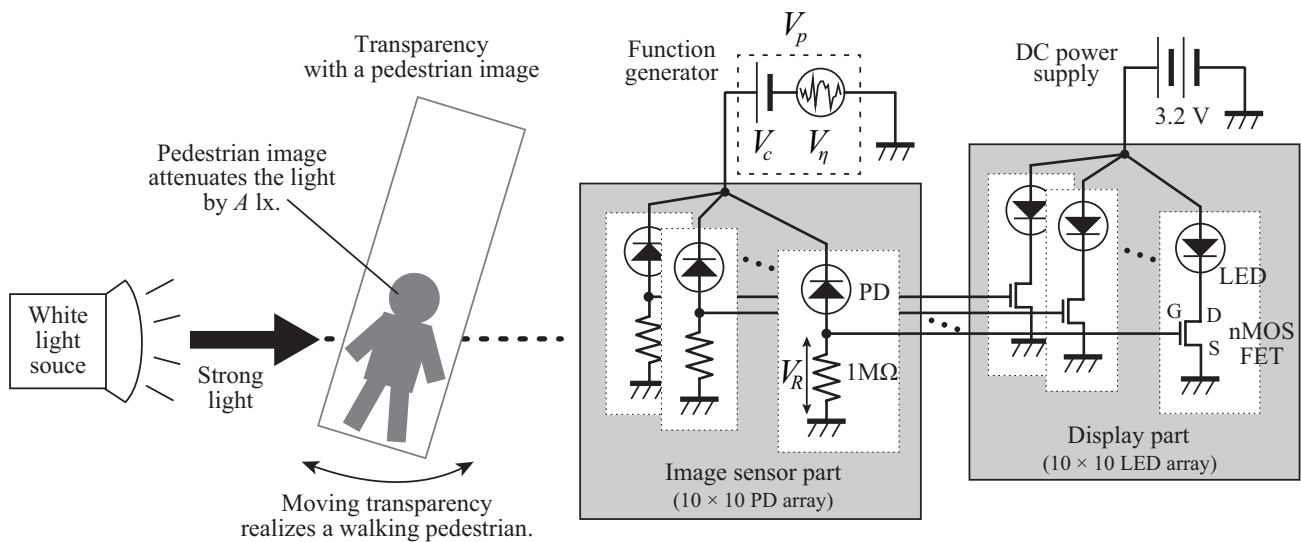

Fig. 2   System model and circuit diagrams of the device.

(a) Image sensor part (10 × 10 PD array)   (b) Display part (10 × 10 LED array)

Fig. 3   Photograph of the device.

arises and the nature of the saturation. When the PD detects light, the photoelectric effect causes a flow of electrical current, reducing the voltage applied to the PD and increasing the voltage V_R applied to the 1 MΩ resistor. Thus, V_R is proportional to the intensity of the light detected by the PD. The brightness of each LED in the display is then proportional to V_R. We first investigated the onset of saturation by measuring the PD voltage as a function of the input light intensity l, and the results are shown in **Fig. 4**. Note that there was no applied noise in this case, so that $V_p = V_c$. The intensity of the input light was measured using an actinometer (Minolta Digital Intensity Meter T-1H) located under the PD. The light intensity was varied by changing the distance between the PD and the LED light source. In Fig. 4, two regions can be seen: a response region (orange) in which V_R increases with the input light intensity and a saturated region (light blue), in which increased light intensity produces no change in V_R. In the latter region, the shape of the pedestrian cannot be properly recognized on the LED display. However, this problem may be solved by increasing the driving voltage to shift the device into the response regime. For example, for an input light intensity of 100 lx, a driving voltage of $V_p = 2.0$ V would correspond to the saturated regime, but increasing V_p to 4.0 V shifts the device into the response regime. Therefore, saturation can be avoided by choosing an appropriate driving voltage.

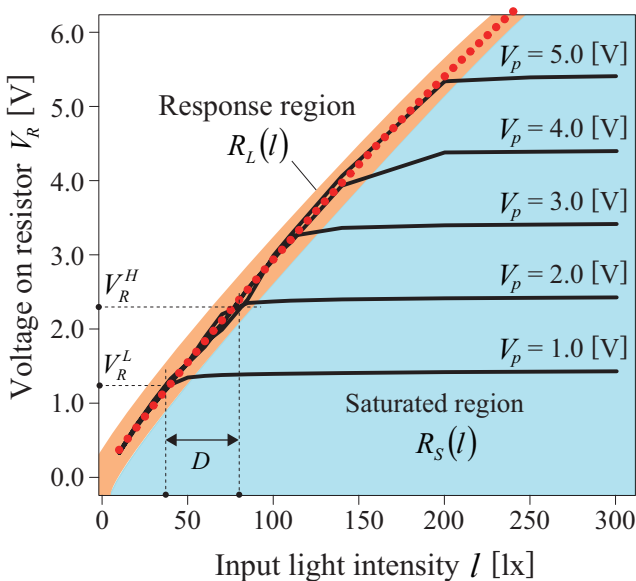In the response regime, the device exhibits identical behavior irrespective of the driving voltage. Fitting the voltage V_R in this region to a polynomial of the form $R_L(l) = \alpha l^2 + \beta l + \gamma$, we find $\alpha = -2.0 \times 10^{-5}$, $\beta = 0.0307$, $\gamma = -0.0750$. The polynomial is indicated by red circles in Fig. 4. The coefficient of determination is 0.9976, which is very close to the ideal value of 1, demonstrating that the quadratic polynomial accurately describes the behavior of the device in the response region. On the other hand, in the saturated region, V_R is independent of light intensity, but instead increases in proportion to the driving voltage. Here, the resistor voltage in this region is given by $R_S(l) = V_p + V_o$ with $V_o = 0.425$. The relation between the voltage V_R and the light intensity l can then be expressed in the form.

$$
\begin{aligned}
V_R &= H(l; V_p) \\
&= \begin{cases} R_L(l) = \alpha l^2 + \beta l + \gamma & (l < l_0) \\ R_S(l) = V_p + V_o & (l \geq l_0) \end{cases}
\end{aligned} \tag{2}
$$

Here, l_0 is the value of l that satisfies $R_L(l) = R_S(V_p)$, i.e., the input light intensity at which the $R_L(l)$ and $R_S(V_p)$ curves intersect:

$$
l_0 = R_L^{-1}(V_p) = \frac{-\beta + \sqrt{\beta^2 + 4\alpha(V_p - \gamma)}}{2\alpha}. \tag{3}
$$

We next consider the relationship between the MOSFET drain-source voltage V_T and the LED voltage V_L. **Figure 5** shows the results of measurements in which the driving voltage was varied at an input light
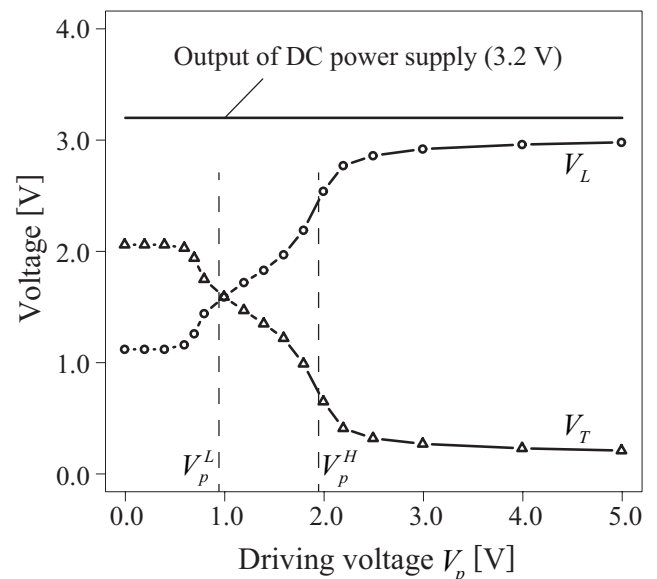

Fig. 4 Resistor voltage V_R for the input light intensity l.

Fig. 5 Measured V_T and V_L for the driving voltage V_p.

intensity of 120 lx. We first see that V_T varies in the range 0.0-2.1 V. From the device data sheet,[16] we know that the output current responds linearly when the voltage V_T is within this range. In other words, the MOSFET is not saturated. Next, regarding the LED voltage V_L, we see that the voltage V_L rises almost linearly with V_p after turning on for values of V_p above 0.7 V; however, V_L saturates when V_p rises above 2.0 V.[15] Thus, for light intensities corresponding to V_L values of 2.0 V or greater, the light pattern received by the PD array cannot be reproduced by the LED array. Denoting the minimum driving voltage at which the LED can operate as V_p^L, and the voltage at which saturation begins as V_p^H, from Fig. 5 we find the values $V_p^L = 0.95$ V and $V_p^H = 1.95$ V.

Finally, from Figs. 4 and 5, the dynamic range D for the prototype device can be determined. First, from the saturated region, the upper and lower threshold voltages are $V_R^H = S(V_p^H)$ and $V_R^L = S(V_p^L)$, respectively; these determine the voltage range within which the LED can respond. Next, from the response region, the corresponding input light intensities can be determined. These are expressed as $l^L = L^{-1}(V_R^L)$ and $l^H = L^{-1}(V_R^H)$ and are calculated using Eq. (3). The dynamic range is then given by $D = l^H - l^L$. In practice, we find $V_p^L \approx 0.95$ V, from which we determine $V_R^L = 1.38$ V and $l^L = 43.6$ lx; similarly, we find $l^H = 79.0$ lx. Thus, the dynamic range in the absence of noise is $D = 35.4$ lx. The intensity of light received by the PD array must lie within this range to be displayed properly by the LED array.

3.2 Performance of the System in the Presence of Added Noise

As discussed in the previous section, LED saturation prevents the display of the input light pattern when the intensity of the light exceeds l^H. We now attempt to improve the dynamic range of the device by stochastically varying the PD characteristics through the addition of noise. In what follows, we present an analytical derivation of the averaged applied voltage on the resistor in the presence of added noise, and assess the resulting increase in the dynamic range.

We assume that the PD driving voltage V_p contains a noise component V_η (so that $V_p = V_\eta + V_c$). Then, using Eq. (2), the averaged applied voltage on the resistor may be written in the form.

$$\bar{V}_R(l; \sigma_\eta^2) = \int_{-\infty}^{+\infty} H(l; V_p) P(V_p) dV_p$$
$$= \int_{-\infty}^{\xi(l)} R_S(V_p) P(V_p) dV_p + \int_{\xi(l)}^{+\infty} R_L(l) P(V_p) dV_p$$
$$(4)$$

Here, $\xi(l)$ is the driving voltage V_p that satisfies $R_L(l) = R_S(V_p)$ – that is, the driving voltage V_p whose corresponding applied voltage in the saturation-region, $R_S(V_p)$, takes the same value as that in the response-region $R_L(l)$ – and may be expressed in the form.

$$\xi(l) = \alpha l^2 + \beta l + \gamma - V_o \qquad (5)$$

Figure 6 shows numerical results for the averaged voltage applied to the resistor, obtained by substituting Eq. (1) into Eq. (4). Here, we set the average value of the driving voltage to $V_c = 2.0$ V and considered three different values for the added noise power (variance). The voltage in the absence of added noise (corresponding to $V_p = 2.0$ V in Fig. 4) is also shown for comparison. For a noise variance σ_η^2, we may express the input light intensity at which the average voltage equals the lower threshold voltage V_R^L in the form, $\bar{l}^L = \bar{V}_R^{-1}(V_R^L)$, where $\bar{V}_R^{-1}$ is the inverse of the function defined by Eq. (4). Similarly, the input light intensity for the upper threshold voltage is given by $\bar{l}^H = \bar{V}_R^{-1}(V_R^H)$. Then the dynamic range in the presence of added noise takes the form.
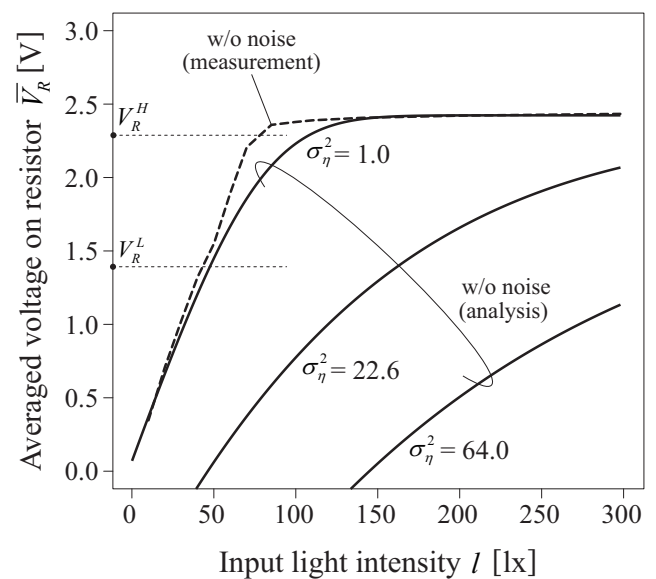

Fig. 6 Average resistor voltage in the case of adding noise.

$$\overline{D} = \overline{l}^H - \overline{l}^L \qquad (6)$$

As discussed in Sec. 3. 1, the intensity of the light received by the detector must fall within this dynamic range – that is, it must lie between $\overline{l}^L$ and $\overline{l}^H$, in order to be displayed by the LEDs. We can conclude the following from Fig. 6:

(i) As the noise power increases, the slope of the response curve is reduced to less than its value in the absence of added noise. Thus, the range of input light intensity for which the system is able to respond without saturation is expanded, yielding an increase in the dynamic range.

(ii) For large noise power, the average voltage for low-intensity input light decreases. Thus, the range of input light intensity that may be properly displayed by the LEDs shifts in the direction of higher intensity, and the system becomes unable to respond to a weak light input.

To clarify points (i) and (ii), **Fig. 7** shows a numerical example of the noise-power dependence of the dynamic range D and the minimum light intensity $\overline{l}^H$ to which the system can respond. It can be seen that both $\overline{D}$ and $\overline{l}^H$ increase with increasing noise power. However, they increase in different ways: at small noise levels, $\overline{D}$ increases rapidly with noise power, while $\overline{l}^H$ increases more gradually. In contrast, at large noise levels, both increase relatively linearly.

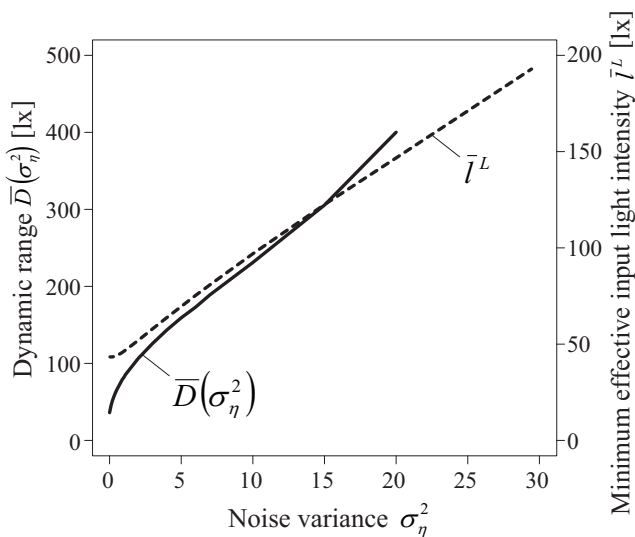As noted in the Introduction, AGC is one method of compensating for the situation shown in Fig. 1.

The method proposed in the present paper allows the dynamic range to be shifted into a desired region, so that the system can accommodate high-intensity input light, and thereby recognize pedestrians. The use of AGC would also allow the minimum effective light intensity to be shifted in a manner similar to that shown in Fig. 7. However, because AGC cannot increase the dynamic range, such a shift would prevent the system from responding to low-intensity input light, resulting in poor recognition performance. As demonstrated by Fig. 7, the stochastic-resonance-based system not only shifts the dynamic range but also increases it, allowing such performance degradation to be avoided.

4. Visual Tests of Improved Recognition Performance through the Addition of Noise

We visually tested the impact on pedestrian recognition performance of our application of stochastic resonance. Because the effect of stochastic resonance depends on the noise power, we treated the noise power level as a variable parameter, and attempted to find the optimum value.

Figure 8 shows the LED display for cases with and without added noise. We adjusted the distance between the LED light source and the detector so that the input light intensity at the PD was 150 lx. Since the light was attenuated by 70 lx by the image printed on the OHP film to mimic a pedestrian, the PD received 80 lx of light in this region. The voltage offset for the PD driving voltage was $V_c = 2.0$ V; we made measurements with no added noise and for three different noise power levels. In the absence of added noise, Fig. 4 shows that for $V_p = 2.0$ V, light intensities of 150 and 80 lx lie outside the dynamic range, and thus the PD saturates. For this reason, the shape of the pedestrian cannot be displayed by the LED array, as shown in Fig. 8(a).

Figures 8(b) to (d) show the results in the presence of added noise. It can be seen that the shape of the pedestrian is most clearly recognizable in Fig. 8(c). This is because intensities of 150 and 80 lx lie within the dynamic range of the device, and the input light pattern is properly displayed by the LEDs. In Fig. 8(b), for a smaller noise power, the shape of the pedestrian cannot be discerned. From the curve for $\sigma_\eta^2 = 1.0$ in Fig. 6, it can be seen that whereas a light intensity of 80 lx lies within the dynamic range, 150 lx does not. As a result, there is effectively no difference in light intensity between the pedestrian region and the

Fig. 7 Dynamic range $\overline{D}$ and minimum effective input light intensity $\overline{l}^L$ for the noise variance.

outer region, and the shape of the pedestrian cannot be discerned. On the other hand, in Fig. 8(d) the noise power is too large, and neither the 150 nor 80 lx component exceeds the minimal effective input light intensity. Consequently, the LED brightness drops to extremely low levels and the shape of the pedestrian cannot be discerned. Based on these findings, we conclude that the addition of an appropriate amount of noise power can improve the system performance in identifying pedestrians. The noise power level that yields the optimal performance improvement is that which ensures that the input light exceeds the threshold level above which the system is able to respond – while simultaneously increasing the dynamic range.

5. Conclusions

In this report, we demonstrated one of the benefits derived from the use of stochastic resonance – namely, the ability to recognize weak signals to which the system could not otherwise respond, by adding an appropriate quantity of noise. We constructed a prototype device to test this effect; by analyzing its properties in detail we provided a clear analytical explanation of the improved dynamic range obtained through the addition of noise. In particular, compared to the existing method of AGC, our proposed technique has the effect not only of shifting the dynamic range but also of increasing it. We obtained visual confirmation of these effects in an experimental system designed to mimic a real-world situation.
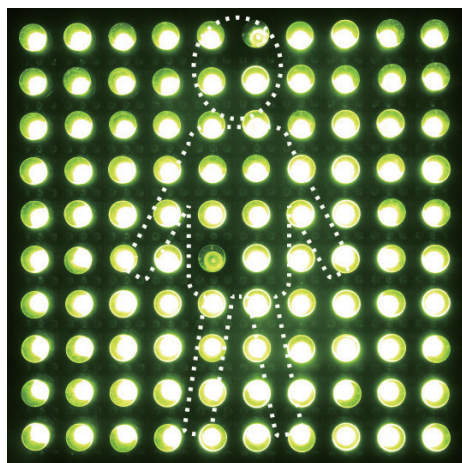
(a) $\sigma_\eta^2 = 0.0$ (no addition of the noise)
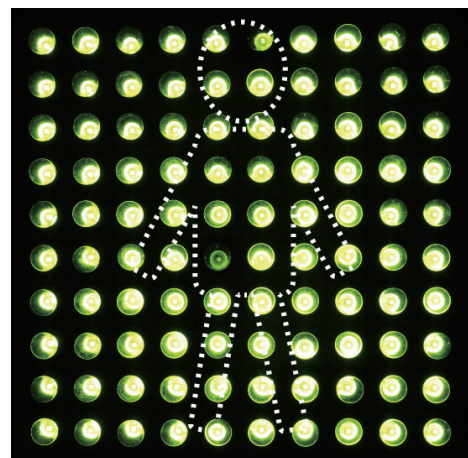
(b) $\sigma_\eta^2 = 1.0$
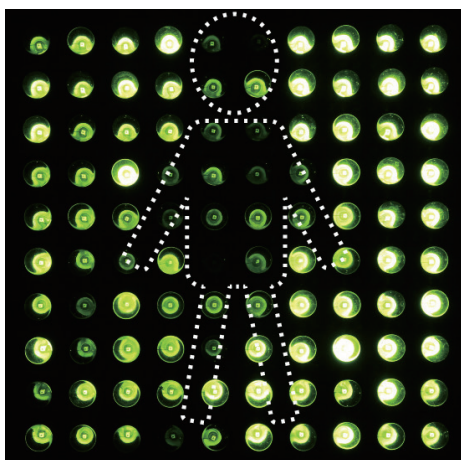
(c) $\sigma_\eta^2 = 22.6$

(d) $\sigma_\eta^2 = 64.0$

Fig. 8　Visual perception of noise-enhanced pedestrian recognition.

Our proposed method is particularly well suited to applications such as night-vision systems in which a situation like that shown in Fig. 1 is captured by a camera or other optical device, subjected to signal processing, and then displayed to facilitate driver recognition. However, because the characteristics of devices exhibiting saturation may generally be modeled in ways similar to that shown in Fig. 4, the topic of our investigation need not be limited to optical applications, but should be broadly applicable to a wide variety of situations. To realize the benefits we have studied in this paper would require the additional installation of noise-generation equipment; future work will consider alternatives to this approach, in addition to real-world environments, such as noise-power calibration methods that adjust to the constantly changing environment of a vehicle in motion.

References

(1) Wiesenfeld, K. and Moss, F., "Stochastic Resonance and the Benefits of Noise: from Ice Ages to Crayfish and SQUIDs", *Nature*, Vol. 373, No. 6509 (1995), pp. 33-36.

(2) McNamara, B. and Wiesenfeld, K., "Theory of Stochastic Resonance", *Phys. Rev. A*, Vol. 39, No. 9 (1989), pp. 4854-4869.

(3) Gammaitoni, L., Hänggi, P., Jung, P. and Marchesoni, F., "Stochastic Resonance", *Rev. Mod. Phys.*, Vol. 70, No. 1 (1998), pp. 223-287.

(4) Dykman, M. I. and McClintock, P. V. E., "What Can Stochastic Resonance Do?", Nature, Vol. 391, No. 6665 (1998), p. 344.

(5) Collins, J. J., Chow, C. C. and Imhoff, T. T., "Stochastic Resonance without Tuning", *Nature*, Vol. 376, No. 6537 (1995), pp. 236-238.

(6) Ichiki, A., Tadokoro, Y. and Takanashi, M., "Sampling Frequency Analysis for Efficient Stochastic Resonance in Digital Signal Processing", *J. Signal Process.*, Vol. 16, No. 6 (2012), pp. 467-475.

(7) Kasai, S. and Asai, T., "Stochastic Resonance in Schottky Wrap Gate-controlled GaAs Nanowire Field-effect Transistors and Their Networks", *Appl. Phys. Express*, Vol. 1, No. 8 (2008), 083001.

(8) Kosko, B. and Mitaim, S., "Stochastic Resonance in Noisy Threshold Neurons", *Neural Netw.*, Vol. 16, No. 5-6 (2003), pp. 755-761.

(9) Ichiki, A. and Tadokoro, Y., "Relation between Optimal Nonlinearity and Non-Gaussian Noise: Enhancing a Weak Signal in a Nonlinear System", *Phys. Rev. E*, Vol. 87, No. 1 (2013), 012124.

(10) Kasai, S., Tadokoro, Y. and Ichiki, A., "Design and Characterization of Nonlinear Functions for the Transmission of a Small Signal with Non-Gaussian Noise", *Phys. Rev. E*, Vol. 88, No. 6 (2013), 062127.

(11) Chapeau-Blondeau, F. and Rousseau, D., "Noise-enhanced Performance for an Optimal Bayesian Estimator", *IEEE Trans. Signal Process.*, Vol. 52, No. 5 (2004), pp. 1327-1334.

(12) Sugiura, S., Ichiki, A. and Tadokoro, Y., "Stochastic-resonance Based Iterative Detection for Serially-concatenated Turbo Codes," *IEEE Signal Process. Lett.*, Vol. 19, No. 10 (2012), pp. 655-658.

(13) Kay, S., "Noise Enhanced Detection as a Special Case of Randomization", *IEEE Signal Process. Lett.*, Vol. 15 (2008), pp. 709-712.

(14) SIEMENS, "Data Sheet: Silicon PIN Photodiode with Very Short Switching Time", No. SFH 229 (1997), 5p.

(15) ROHM Semiconductor, "Data Sheet: SLR-56 Series", (2010), 7p.

(16) Diodes Inc., "Data Sheet: ZVN2110A Series", (1994), 3p.

Yukihiro Tadokoro
　Research Field:
　　- Nanostructured Signal Processing
　　　System, Noise-induced System,
　　　Data Mining for Control System and
　　　Bio-informatics
　Academic Degree: Dr.Eng.
　Academic Societies:
　　- IEEE
　　- The Institute of Electronics, Information and
　　　Communication Engineers

Hiroya Tanaka
　Research Field:
　　- Nanostructured Electromagnetic
　　　Devices
　Academic Degree: Dr.Eng.
　Academic Society:
　　- IEEE

* Hokkaido University

Seiya Kasai*
　Research Fields:
　　- III-V Compound Semiconductor
　　　Nanodevices and Their Integration
　　- Nonlinear Phenomena in Electron
　　　Devices
　Academic Degree: Dr.Eng.
　Academic Societies:
　　- IEEE
　　- The Institute of Electronics, Information and
　　　Communication Engineers
　　- The Japan Society of Applied Physics
　Awards:
　　- SSDM Young Researcher Award, The Japan Society
　　　of Applied Physics, 1996
　　- JSAP Young Scientist Presentation Award, The Japan
　　　Society of Applied Physics, 2000
　　- Poster Prize, NGC (Nano and Giga Challenges in
　　　Electronics and Photonics), 2007
　　- Award for Outstanding Paper, MNC
　　　(Int. Microprocesses and Nanotechnology Conf.),
　　　2007, 2010, 2013

Akihisa Ichiki
　Research Field:
　　- Stochastic Process, Non-equilibrium
　　　Physics and Noise-induced
　　　Phenomena, and Their Applications
　　　Including Machine Learning
　Academic Degree: Ph.D.
　Academic Society:
　　- The Physical Society of Japan
　Present Affiliation: Nagoya University